journal

J. Am. Ceram. Soc., 92 [5] 990–995 (2009)
DOI: 10.1111/j.1551-2916.2009.02959.x

The Effect of Conformation Method and Sintering Technique on the Densification and Grain Growth of Nanocrystalline 8 mol% Yttria-Stabilized Zirconia

Mehdi Mazaheri,[†,‡,§] Z. Razavi Hesabi,[§] F. Golestani-Fard,[¶] S. Mollazadeh,[§] S. Jafari,[§] and S. K. Sadrnezhaad[§]

[§]Materials and Energy Research Center, P.O. Box 14155-4777, Tehran, Iran

[¶]Department of Materials and Metallurgical Engineering, Iran University of Science and Technology, Tehran, Iran

Uniaxial dry pressing (DP) and slip casting (SC) were used to form green bodies of nanocrystalline 8 mol% yttria-stabilized zirconia powder processed via the glycine-nitrate combustion method. The SC method was shown to be a more efficient, yielding more homogenous green bodies with higher green density (60% theoretical density) which contained smaller pores with narrower distribution. Improved green properties resulted in lowering the sintering temperature of SC bodies by about 200°C compared with DP compacts. Consequently, the grain growth in sintered bodies formed by SC was relatively abated. By taking the benefits of the wet conformation method, the final grain size of nearly full dense (>97% TD) structures was reduced by 39% (i.e. from 2.15 to 1.3 μm). To reveal the effect of sintering technique, DP bodies were sintered via both microwave and two-step sintering methods. While the grain size of two-step sintered samples was <300 nm, sintering via microwave radiation yielded a nearly full dense structure with a mean grain size of 0.9 μm. The results show that conventionally sintered SC bodies posses higher indentation fracture toughness (FT) (~3 MPa·m$^{1/2}$) compared with DP samples (1.6 MPa·m$^{1/2}$). Interestingly, it was shown that, without applying any modified sintering technique, the hardness and FT of SC bodies with coarser structures are completely close to those of samples sintered via microwave heating.

I. Introduction

Among different types of ceramics, 8 mol% yttria-stabilized zirconia (8YSZ), because of its high oxygen ionic conductivity and chemical stability over a wide range of temperature, is a well-known candidate for oxygen sensors, oxygen pumps, and oxide fuel cells.[1–3] Although 8YSZ possesses high ionic conductivity, low mechanical properties (such as fracture toughness (FT)) limit its application, especially when thermal and mechanical stresses are applied under service condition. To enhance mechanical properties, one can use grain refining. To attain this goal, using nanopowders has attracted much attention recently.[4,5] Although using nanopowders offers the possibility of manufacturing dense ceramics at lower sintering temperatures, leading to the formation of finer structures, homogenous green bodies are required.[1] The agglomeration of nanoparticles can result in the formation of flaws, deteriorating the mechanical properties of sintered structures.[6] In order to overcome the interactive forces among nanoparticles and produce homogenous green bodies, one can use wet conformation methods. For instance, Vasylkiv *et al.*[4] shaped zirconia nanopowder via slip casting (SC). They showed that densification at lower temperatures was possible, just when a highly uniform packing of the nanoaggregates was achieved in the green compacts. Shan and Zhang[7] reported that a significantly low green density and large linear shrinkage are the characteristics of the casted bodies of slurries containing nanometric powder. They achieved a maximum green density of about 37% theoretical density (TD) when 53 wt% of solid content was used. Zhang *et al.*[8] produced bodies with a relative green density of ~35% TD by SC of slurries with 53 wt% ZrO_2–15 vol% Al_2O_3 nanopowder. Although there are many reports about SC of nanopowders, the literature has not distinctly reported the efficiency of wet conformation methods in comparison with conventional dry pressing (DP).

In addition to the conformation method, the sintering technique can have considerable influence on the densification and grain growth of nanopowders. For instance, Dahl *et al.*[9] sintered the pressed 8YSZ nanopowder (around 50 nm) by conventional pressureless sintering (CS) and the hot pressing method (HP) at 1500° and 1250°C, respectively. They have reported that the final grain size of nearly full dense (>96% TD) samples produced via the HP method is 32 times less than that of the CS method. While the hardness of sintered samples was found to be independent on grain size, the FT decreased with increasing grain size.[9] Interestingly, Chen and Wang[10] showed that without applying any external force during the sintering of nanopowders, the grain growth would be suppressed significantly through two-step sintering (TSS) method. Fast firing through microwave heating was reported as another efficient technique for hindering the grain growth as well as producing a homogenous microstructure.[11] Referring to the open literature, the effect of conformation method and sintering technique has not yet been systematically investigated where a ceramic nanopowder is used.

In the present study, nanocrystalline 8YSZ powder was synthesized via the glycine-nitrate combustion method. As-synthesized powder was conformed via the uniaxial dry pressing and slip casting methods. The importance of conformation method on particle coordination was explained via pore distribution in green samples. Additionally, in order to reveal the effect of the green state on the sintering path and obtainable mechanical properties, densification, microstructural evolution, hardness, and indentation FT of samples produced by DP and SC were compared. In order to distinguish the effect of sintering technique from the conformation method, microwave heating and two-step sintering were applied on the DP samples. To have a better insight on the conformation technique and sintering method of 8YSZ nanopowder, the sintering paths for different methods were compared.

C.-H. Hsueh—contributing editor

Manuscript No. 24926. Received July 1, 2008; approved December 23, 2008.
[†]Author to whom correspondence should be addressed. e-mail: mmazaheri@gmail.com; mehdi.mazaheri@epfl.ch

[‡]Present address: EPFL: Swiss Federal Institute of Technology in Lausanne SB-IPMC-LNNME, PH D2 434 (Batiment PH) Station 3, CH-1015 Lausanne, Switzerland.

II. Experimental Procedure

(1) Powder Synthesis and Characterization

Nanocrystalline powder of 8YSZ was synthesized through the glycine-nitrate combustion process. Zirconyl nitrate ($ZrO(NO_3)_2 \cdot 6H_2O$) and yttrium nitrate ($Y(NO_3)_3 \cdot 6H_2O$) (Aldrich, Buchs, Switzerland) were used as oxidizers (starting materials) with an elemental stochiometric coefficient of $\Phi = 1.163$. These were dissolved in deionized water at 40°C, and then glycine ($C_2H_5O_2N$) (Merck, Darmstadt, Germany), as a motivator of the combustion process (fuel), was added to the resulting solution. The theoretical stochiometric reaction formulation for complete combustion may be written as follows (Eq. (1)):

$$0.84ZrO(NO_3)_2 + 0.16Y(NO_3)_3 + 1.2C_2H_5O_2N \rightarrow Zr_{0.84}Y_{0.16}O_{1.92} + 2.4CO_2 + 9H_2O + 1.68N_2 \quad (1)$$

The pH of the solution was adjusted to 3 through NH_4OH addition. The obtained solution was thermally dehydrated at 90°–100°C on a hot plate until a highly viscous transparent gel-like precursor was obtained. The beaker vessel was then transferred into a muffle furnace preheated to 350°C. The products were calcined for 2 h at 700°C with a heating rate of 10°C min^{-1} in an air atmosphere in a tube furnace in order to get rid of unreacted materials. The details of the synthesis procedure were reported previously.[5,12] The as-synthesized sheet-like nanocrystalline agglomerates were milled in a planetary ball mill in order to break foamy agglomerates. The milling was conducted in an isopropanol medium using zirconia balls at a rotational speed of 200 rpm. The milled powder was dried in air at 60°C for 24 h. Transmission electron microscopy (TEM, CM 200 FEG, Philips, Eindhoven, the Netherlands) and the Brunauer-Emmett-Teller (BET, Micromeretics Gemini 2375, Norcross, GA) method were utilized to determine the particle size and surface area of the as-milled powder, respectively.

(2) Conforming Green Bodies

Green bodies were conformed by two different methods of DP and SC. The uniaxial pressing was performed at different pressures in a steel cylindrical die (10 mm diameter) in order to shape the pellets. The green pellets were characterized by density measurement using the volumetric method. For measuring the weight and dimensions of the compacts, an accurate balance (10^{-5} g) and a micrometer caliper (10^{-5} m) were used. For SC, aqueous slurries with different solid contents (42–67 wt%) and a fixed amount (0.8 wt% solid) of Dolapix (CE64, Zschimmer & Schwarz, Lahnstein, Germany), used as a sterical stabilizer of the slurry, were prepared. The pH of the suspensions was adjusted to 3 by adding HNO_3. The pellets were formed by pouring the suspensions into plaster molds followed by drying in an oven at 110°C for 24 h. To study the pore size distribution of green bodies formed via SC and DP, the Mercury porosimetry method was used. In order to avoid sample breakage during the porosimetry test in mercury, pre-sintering was performed by heating the green samples at 800°C. At this temperature, the formation of necks gives the green bodies micromechanical stability. The first shrinkage during the heating of green bodies to 800°C, however, is so small (<0.5%) that the original green porosity is retained and this state was representative of the green state.

(3) Sintering

To show the effect of the conformation method on densification behavior, green bodies formed via DP and SC were conventionally sintered up to 1500°C, with a heating rate of 5°C min^{-1} with no holding. In order to investigate the effect of the sintering technique, samples pressed at 600 MPa with the highest relative density (~48% TD) were sintered through microwave heating as well as through the two-step sintering method. Microwave sintering (MS) was conducted in a 1.1 kW, 2.45 GHz multimode microwave cavity (Bosch, Stuttgart, Germany). Details of the MS procedure were previously reported by Mazaheri *et al.*[11] Similar to CS, MS was conducted up to 1500°C with a significantly higher heating rate of 50°C min^{-1}. TSS was conducted via heating to 1250°C with no holding, followed by cooling down to 1050°C and prolonged soaking for 20 h at 1050°C. The densification behavior of used powder in the present study through TSS was investigated in detail, previously.[5] The density of sintered pellets was measured by the Archimedes method. The microstructural features were inspected by scanning electron microscopy (SEM, Philips XL30). In order to investigate sample microstructure, sintered pellets were polished and then thermally etched at a temperature 50°C lower than the fired temperature. The grain size of the sintered samples was determined by multiplying the average linear intercept by 1.56.[13] For each specimen, at least 15 lines were taken, and their average was reported.

(4) Mechanical Properties

Hardness (H_v) was calculated using the Vickers indentation method on the polished surface of the sintered samples. The indents were made with an applied load of 5 kg for 20 s and measured by SEM. H_v was calculated using the following equaiton:[14]

$$H_V = \frac{1.854P}{d^2} \quad (2)$$

where P is the applied load and d is the mean value of the diagonal length. Also, FT (K_{IC}) was determined using the following equation:[15]

$$K_{IC} = 0.0016\left(\frac{E}{H_V}\right)^{1/2}\left(\frac{P}{C^{3/2}}\right) \quad (3)$$

where C is the crack length emanating the indentation center and E is the Young modulus.

III. Results and Discussion

(1) Powder Characterization

A TEM micrograph of the as-milled 8YSZ nanopowder is displayed in Fig. 1. As shown, even after mechanical milling, agglomerates can be observed. The observed rings in the selected area diffraction pattern of the sample (aperture size of 100 nm), embedded in Fig. 1, confirm the nanocrystallinity of the powder. Table I summarizes the average crystallite size, particle size, and surface area of the nanoparticles. As seen, the particle size of the powder calculated by BET data is in good agreement with TEM analysis.

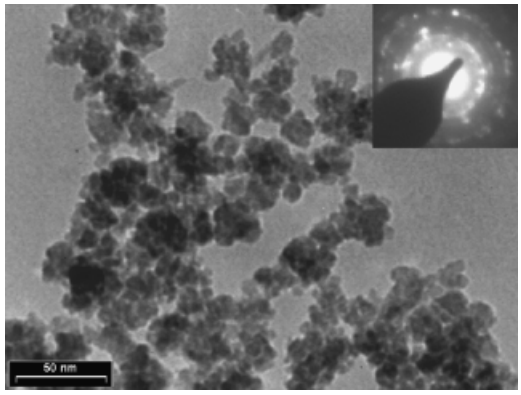

Fig. 1. TEM image of nanocrystalline 8 mol% yttria-stabilized zirconia (8YSZ) powder synthesized via the glycine-nitrate method after milling for 24 h.

Table I. Characteristics of Nanocrystalline 8 mol% Yttria Stabilized Zirconia Powder Synthesized by the Glycine-Nitrate Combustion Method

Surface area ($m^2\ g^{-1}$)	Particle size (nm)		Grain size† (nm)	Phase
41.2	BET	TEM	10.20	Cubic
	24.5	15–33		

†Calculated using the Scherer equation.

(2) The Effect of Conformation Method

Figure 2 shows the fractional green density of dry pressed and SC bodies as a function of applied pressure (in a logarithmic scale) and solid load (wt%), respectively. As shown, with increasing the solid content, a continuous increase in green density was observed, while in DP, two break points (P_y and P_c) separate three distinct lines. The first break point (P_y) has been reported to be the strength of the agglomerates of the starting powder.[16,17] A significant increase in density was achieved above P_y (370 MPa), where agglomerates were fragmented and rearranged. The upward trend was ceased at 600 MPa, in which a further increase of pressure did not increase the green density. The inspection of green bodies revealed the occurrence of lamination transverse to the load direction at higher pressures (e.g. 900 MPa). The maximum green density of sound, dry pressed bodies was ~48% of the TD.

As shown in Fig. 2, the SC of slurry containing ~65 wt% of nanocrystalline powder led to the formation of green bodies with a relative green density of ~60% TD. It is interesting that a SC body of nanopowder demonstrates a higher green density compared with a pressed one. It seems that in SC, nanoparticles rearrange and slide over each other freely and yield a better compaction. Table II compares the green density of SC nanopowders/nanocomposites reported previously with that of the present study. As seen, in the present study the higher green density was obtained. The higher solid content of 65 wt% in the present study may be responsible for the higher density. However, the results show that in an identical solid content, for instance ~53 wt%, the relative density in the present work reached ~46% TD while Zhang *et al.*[8] reported a TD of only 36%. In other words, the relative density of SC bodies in the present study increased more than 20% in comparison with those reported before.[8] The authors believe the high green density of SC 8YSZ nanopowder can be related to the better influence of dispersant used in the current work and to the fragmentation of large agglomerates to smaller ones through mechanical milling.

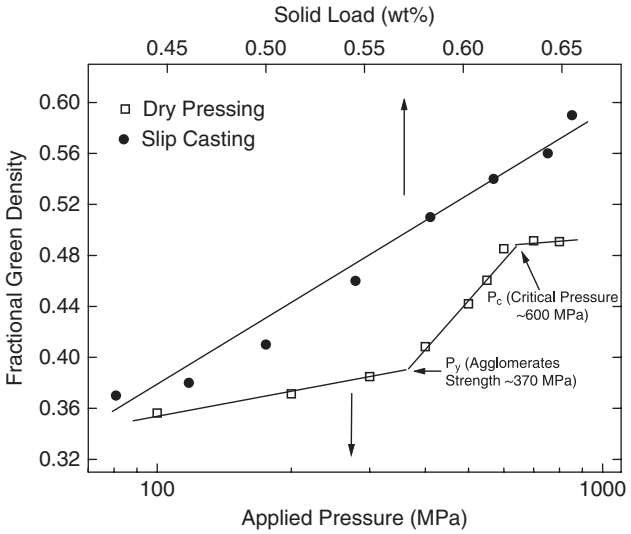

Fig. 2. The effect of applied pressure and solid load on the fractional green density of nanocrystalline 8 mol% yttria-stabilized zirconia (8YSZ) compacts conformed by DP and SC, respectively.

Table II. Green Density of Different Ceramic Nanopowders Conformed through Slip Casting

	Nanopowder /Nanocomposite	Solid content	Green density (% TD)
Zhang *et al.*[8]	ZrO_2/Al_2O_3	53 wt%	36
Santos *et al.*[18]	Ce–ZrO_2	13.9 vol%	35
Shan *et al.*[7]	ZrO_2	55 wt%	37
Present study	8 mol% yttria-ZrO_2	65 wt%	60

Another noticeable point is that the green density of dry-pressed samples in the present study is higher than that of the SC samples reported by others.[7,8] The higher densification tendency of the powder used in the present study may be related to the characteristics of powder synthesized by the nitrate combustion method. Sound judgment on this issue demands a study of the surface chemistry of primary particles, which is beyond the scope of the present work.

The densification behavior of nanopowder compacts prepared by DP and SC has not been compared in the literature.[4,7,8,18–20] However, here we can see that while the DP samples reach only 48% TD, the SC bodies experience a 60% TD. In DP, the external forces can hardly move an individual particle into the voids available nearby.[6,21] Thus, uniform packing of nanopowders by DP needs extremely high pressures to overcome huge forces rising from the particles' friction. But the wet conformation processes provide particles the freedom to find their optimum positions on their own. To have a better insight on the effect of the conformation method on the densification behavior of a nanopowder, one can notice the slope of compressibility curves. As Fig. 2 shows, before P_y the densification rate of the DP method is lower than that of the SC one, while above P_y an inverse trend can be observed. As reported previously,[5] a pressure lower than the agglomerate strength (370 MPa) was insufficient to break and rearrange agglomerated particles. Whereas, in the SC procedure, modification of the surface charge of the powders led to deagglomeration of particles. It seems that the powder prepared by the glycine-nitrate combustion method posseses a surface charge that overcomes the attractive forces between nanoparticles and limits the agglomeration of nanoparticles. Study of the surface characteristics of such powders, of course, needs further investigation. In DP it was observed that while reaching the agglomerate strength, a rapid densification occurred, which resulted in the maximum green density of 48% TD at 600 MPa. It is noticeable that even with a lower densification rate, SC with a lower solid content led to a higher green density (Fig. 2). Again, it emphasizes that SC, in terms of reaching higher densities, demonstrates a higher efficiency for the current material.

In order to reveal the effect of the conformation method on sintering behavior, the specimens with the maximum green density shaped through SC (solid load of 65 wt%) and DP (at 600 MPa) were used. Figure 3 shows the fractional fired density of samples as a function of sintering temperature. The sintering curve of pressed samples shows a sigmodal shape, while a linear curve for SC ones was obtained. For DP samples, a slight increase in density was obtained below 1100°C. The rate of sintering increases more rapidly at 1150°–1300°C, at which samples reach 82% TD. In other words, a 150°C increase in temperature (from 1150° to 1300°C) resulted in a 20% increase in density (from 72% to 92% TD). An increase in temperature from 1300° to 1500°C resulted in a slight density enhancement up to 5% (from 92% to 97% TD). A slow sintering rate at the final stage (TD > 90%) could be related to the insoluble pressure gas in residual pores, which can hinder densification mechanisms such as grain-boundary as well as volume diffusion.[17,22]

The densification of nano-8YSZ powder formed by SC as demonstrated in Fig. 3 shows a different behavior. The fractional fired density of SC bodies is significantly higher than that of pressed compacts sintered at an equivalent temperature. For

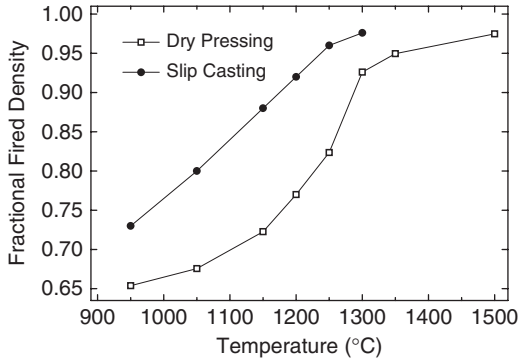

Fig. 3. Fractional fired density as a function of sintering temperature for dry-pressed and SC bodies conventionally sintered up to 1500°C with a constant heating rate of 5°C min^{-1}. The specimens with the maximum green density of 60% TD for slip casting bodies and 48% TD for dry-pressed ones were used.

instance, the fired density of SC samples sintered at 1250°C reached ~96% TD, while the DP samples could only densify to 82% TD. In order to obtain an identical density, sintering of SC bodies requires significantly lower temperatures. Referring to the literature[21] and present results (Fig. 2), the difference in densification behavior is mainly related to the higher green density of SC bodies. Also, the more homogenous particle arrangement in SC bodies may play a role in setting up a smooth densification with a constant rate.

To gain better insight on the sintering behavior of green bodies shaped differently, one can consider the density of samples (with an identical green density) sintered by heating up to 1500°C. Figure 4 shows the fractional fired density of DP samples and SC bodies as a function of fractional green density. It demonstrates that even with an identical green density, the SC bodies exhibit better sinterability compared with DP ones. To investigate this phenomenon, the pore size distribution of bodies with the same green density of 41% TD prepared by DP (at 400 MPa) and SC (with a solid load of ~50 wt%) are compared in Fig. 5. Two distinct differences are distinguished. While large pores up to 375 nm can be found in DP samples, the size of the largest pores formed in SC bodies is less than 80 nm. Also, a narrower pore size distribution in SC bodies is distinguished from the curves in Fig. 4. Wide pore size distribution in DP samples can originate from agglomeration of particles, which imposes poor particle coordination.[6,21,23] Larger pores through green bodies can result in locally different shrinkage in subsequent sintering. Also, this can lead to the higher sintering temperature of DP bodies as explained before. Figure 6 shows the SEM typical micrograph of DP and SC after being sintered at 1500° and 1300°C, respectively. While the average grain size of the DP sample is ~2.15 μm, the wet-shaped 8YSZ body yields a finer texture of ~1.3 μm.

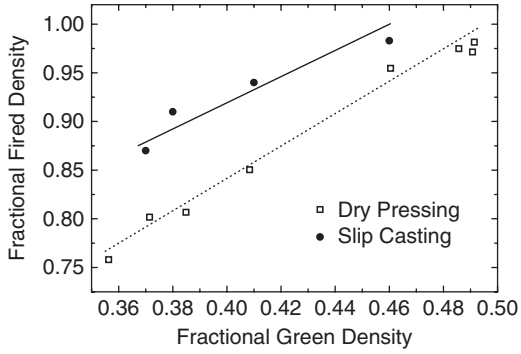

Fig. 4. The fractional fired density of dry-pressed and slip casting bodies as a function of fractional green density. All of the samples were sintered through heating up to 1500°C with the heating rate of 5°C min^{-1}.

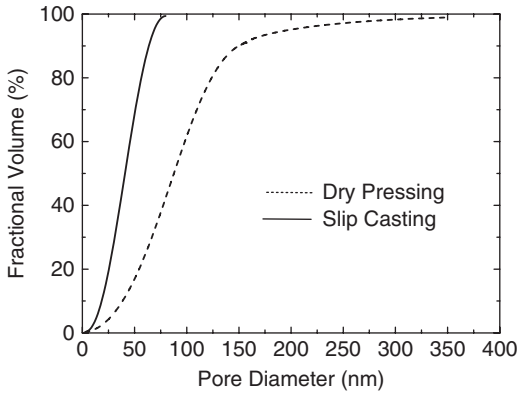

Fig. 5. Pore size distribution of nanocrystalline 8 mol% yttria-stabilized zirconia (8YSZ) compacts formed through dry pressing (pressed at 400 MPa) and slip casting (with a solid load of ~0.50 wt%) with an identical green density of 41% TD. Green samples were pre-sintered at 800°C.

(3) Effect of Sintering Technique

Figure 7 shows the effect of sintering technique (conventional versus microwave sintering) on the densification of pressed 8YSZ nanopowder as a function of sintering temperature. Both densification curves show a sigmoidal shape, and there is not any significant difference between the fractional fired densities of samples sintered conventionally with those prepared by microwave heating. The authors have previously reported that the effect of MS on the densification of 8YSZ nanopowders depended on the heating rate used through the sintering procedure.[11] Figure 8 shows the change of grain size with sintering temperature for samples sintered through conventional and microwave heating. As seen, a remarkable suppression in grain growth is obtained in MS. Sintering by microwave radiation

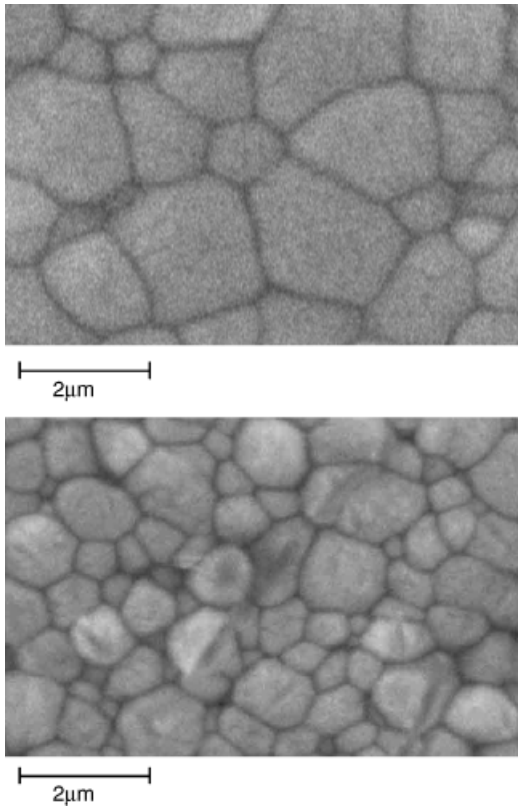

Fig. 6. SEM micrographs of nanocrystalline 8 mol% yttria-stabilized zirconia (8YSZ) compacts conformed by dry pressing and slip casting after conventional sintering at 1500° and 1300°C, respectively. The heating rate was 5°C min^{-1}.

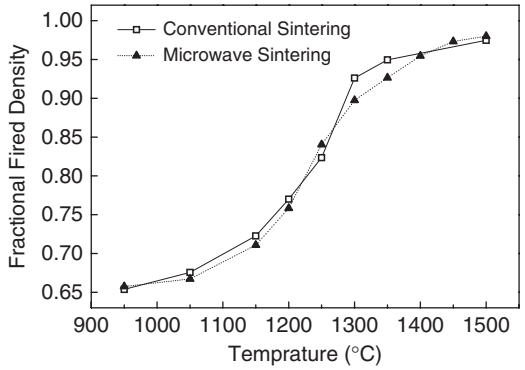

Fig. 7. Fractional fired density versus sintering temperature of dry-pressed nanocrystalline 8 mol% yttria-stabilized zirconia (8YSZ) after conventional and microwave sintering. The heating rate for conventional sintering and MS was 5 and 50°C min^{-1}, respectively.

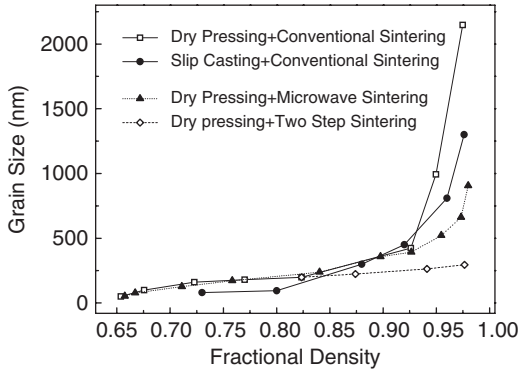

Fig. 9. The effect of the conformation method as well as sintering technique on the sintering paths of nanocrystalline 8 mol% yttria-stabilized zirconia (8YSZ) compacts. Two-step sintering and microwave heating were conducted on green samples conformed by dry pressing.

decreased the mean grain size to 0.9 μm compared with 2.15 μm for conventional sintering. The higher heating rate used in MS results in grain refining, as can be realized from Fig. 8. Also, the fast firing through this method postpones access to the activation energy required for grain boundary mobility. Consequently, a remarkable amount of absorbed energy during microwave heating is consumed for densification and not grain coarsening. The authors have recently shown the effect of TSS on the structural evolution of nanocrystalline 8YSZ. It was demonstrated that by applying the TSS method, the grain size was decreased <300 nm. Pinning of grain boundaries by immobile triple junctions was found to play the main role in suppression of grain growth.[5,13]

To find how efficiently the conformation method as well as the sintering technique would influence the densification and grain growth of a nanopowder, one can consider the sintering path (grain size vs fractional density). Figure 9 represents the sintering paths of nanocrystalline 8YSZ bodies formed by SC and DP with the maximum obtainable green density. The results of DP bodies sintered via microwave heating and the two-step sintering method were also added. As shown, the parabolic grain growth at the final stage of sintering ($TD>90\%$) in conventionally sintered bodies that were shaped differently was observed, but this exaggerated grain growth in SC bodies is more moderate than in DP compacts. The application of a better conformation method, i.e. SC, in order to obtain bodies with a higher green density resulted in an increase in densification kinetic (Figs. 3 and 4). However, grain growth is not generally related to the conformation method. Also, the effect of the conformation method is more effective in systems where the grain growth rate relative to the densification rate is high, such as in DP samples (Fig. 9). As the densification rate is enhanced by higher green density and finer residual pores (Fig. 5) through green bodies, sintering temperature as well as sintering time can be reduced (Fig. 3) and grain growth further suppressed (Fig. 9), for instance sintering temperatures of SC bodies were decreased 200°C compared with DP compacts. As presented in pervious publications,[5,22,24] the efficiency of the TSS method for controlling grain growth during densification at the final stage of sintering is significant. As shown in Fig. 9, no parabolic growth was observed in TSS.[5] The lower temperature in the second step of TSS suppresses the accelerated grain growth. The immobile triple point junctions at the second sintering temperature pin grain boundaries, while grain boundary diffusion is active.[10] MS shows a similar trend, such as in conventionally sintered SC bodies. Seemingly, the effect of SC is similar to that of MS. Shorter sintering time as well as fast firing led to an increase of densification rate to grain growth rate.

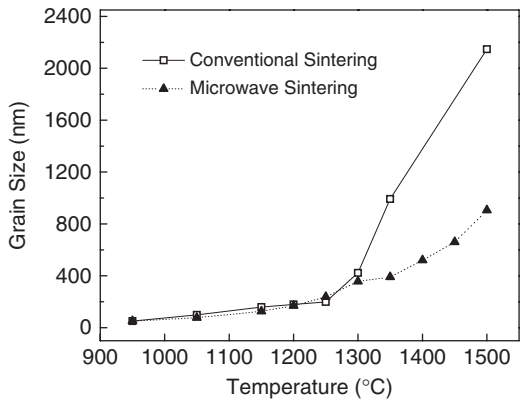

Fig. 8. Grain size versus sintering temperature of dry-pressed nanocrystalline 8 mol% yttria-stabilized zirconia (8YSZ) after conventional (with a heating rate of 5°C min^{-1}) and microwave (with a heating rate of 50°C min^{-1}) sintering.

(4) Hardness and Fracture toughness

Hardness and fracture toughness (FT) of nearly full dense samples are summarized in Table III. As seen, there is no significant change in hardness with varying grain size. However, DP samples that were conventionally sintered show the minimum hardness. This observation confirms the strong effect of final density and available porosity on the hardness of the sintered specimens.[25] The hardness range of the samples (12.8–13.7 GPa) produced through different methods in the present study is close to the available results addressed by other investigators (8.5–13.5 GPa).[17,26–28] The results show that not only the hardness but also the FT of sintered samples does not show strong dependency on grain size. As shown in Table II, the FT values increased from 1.61 (for CS) up to 3 $MPa \cdot m^{1/2}$ (for SC, MS, and TSS). In other words, the SC samples demonstrate a FT value which usually can be expected for TSS or MS. For TSS samples, this behavior can be attributed to the refining of microstructure, which is a well-known method for enhancing the mechanical properties of YSZ bodies.[29] The behavior was at-

Table III. Mechanical Properties of Nearly Full Dense 8 mol% Yttria Stabilized Zirconia (8YSZ) Specimens Processed via Different Methods

Processing method	Fractional density (%)	Grain size (μm)	Hardness (GPa)	Fracture toughness (MPa $m^{1/2}$)
CS[†]	97.4	2.15	12.87	1.61
SC[‡]	97.6	1.3	13.5	3.01
TSS[§]	97.6	0.295	13.5	3.16
MS[¶]	98	0.9	13.72	3.17

[†]Dry pressing+conventional sintering. [‡]Slip casting+conventional sintering. [§]Dry pressing+two-step sintering. [¶]Dry pressing+microwave sintering.

tributed to the better effectiveness of grain boundaries as obstacles against deformation when the grain size is finer.[6] The difference between FT of the nearly full dense bodies sintered through TSS and CS could be referred as microstructural refining. This issue, however, requires further investigations on the microstructure of the bodies.

Based on the present results, we may only conclude that the grain size reduction in CS and SC bodies from 2.15 to 1.3 μm, respectively, as well as the higher homogeneity of SC green bodies along with small residual pores, is responsible for the better FT of SC bodies. This conclusion could be supported by previous studies, in which such particle size distribution was reported to be the main cause for lower shrinkage.[21,23]

The authors previously reported the same reason (higher microstructural homogeneity[11]) for the higher FT of microwave-sintered samples.

IV. Conclusion

The effect of the conformation method (dry pressing and slip casting) as well as sintering technique (conventional sintering, two-step sintering, and microwave sintering) on the densification and grain growth of nanocrystalline 8YSZ powder was investigated. The following results were obtained:

(1) The maximum obtainable green density of dry-pressed samples was 48% of the TD at 600 MPa, while SC of slurry containing 65 wt% 8YSZ nanopowder led to a 12% increase in green density ($\sim$60% TD).

(2) Higher green density of SC samples, finer pores (80 vs 375 nm), and narrower size distribution enabled the SC bodies to be sintered at a temperature $\sim$200°C lower than DP ones. Larger grain size of DP samples (2.15 μm) in comparison with finer grains of SC bodies (1.3 μm) is in good agreement with lower sintering temperature.

3) By pinning of grain boundaries via immobile triple junctions in the two-step sintering method, grain growth at the final stage of sintering was significantly suppressed. Nearly full dense bodies with a grain size of $\sim$300 nm were obtained, while fast densification via MS resulted in a full dense sample with an average grain size of $\sim$0.9 μm.

4) Higher FT of conventionally sintered SC samples (3 $MPa \cdot m^{1/2}$) relative to DP ones (1.6 $MPa \cdot m^{1/2}$) was related to more textural uniformity, while a significant reduction of grain size via two-step sintering was considered as the main cause of improvement in FT.

Acknowledgments

The first author (M. M.) would like to give special gratitude to his fiancee, PARISA, whose patient love enabled me to complete and publish this work.

References

[1]C. Laberty-Robert, F. Ansart, C. Deloget, M. Gaudon, and A. Rousset, "Dense Yttria Stabilized Zirconia: Sintering and Microstructure," *Ceram. Int.*, **29** [2] 151–8 (2003).

[2]T.-H. Yeh and C.-C. Chou, "Doping Effect and Vacancy Formation on Ionic Conductivity of Zirconia Ceramics," *J. Phys. Chem. Solids*, **69** [2–3] 386–92 (2008).

[3]M. Han, X. Tang, H. Yin, and S. Peng, "Fabrication, Microstructure and Properties of a YSZ Electrolyte for SOFCs," *J. Power Sources*, **165** [2] 757–63 (2007).

[4]O. Vasylkiv, Y. Sakka, and V. V. Skorokhod, "Low-Temperature Processing and Mechanical Properties of Zirconia and Zirconia–Alumina Nanoceramics," *J. Am. Ceram. Soc.*, **86** [2] 299–305 (2003).

[5]M. Mazaheri, M. Valefi, Z. R. Hesabi, and S. K. Sadrnezhaad, "Two-Step Sintering of Nanocrystalline $8Y_2O_3$ Stabilized ZrO_2 Synthesized by Glycine Nitrate," *Ceram. Int.*, **35** [1] 13–20 (2009).

[6]A. Krell and P. Blank, "The Influence of Shaping Method on the Grain Size Dependence of Strength in Dense Submicrometre Alumina," *J. Eur. Ceram. Soc.*, **16** [11] 1189–200 (1996).

[7]H. Shan and Z. Zhang, "Slip Casting of Nanometer Sized Tetragonal Zirconia Powder," *Br. Ceram. Trans.*, **95** [1] 35–8 (1996).

[8]Z. Zhang, L. Hu, and M. Fang, "Slip Casting of Nanometer- Sized Powders," *Am. Ceram. Soc. Bull.*, **75** [12] 71–4 (1996).

[9]I. K. P. Dahl, Z. Zhao, M. Johnsson, M. Nygren, K. Wiik, T. Grande, and M. A. Einarsrud, "Densification and Properties of Zirconia Prepared by Three Different Sintering Techniques," *Ceram. Int.*, **73** [8] 1603–10 (2007).

[10]I. W. Chen and X. H. Wang, "Sintering Dense Nanocrystalline Oxide With-Out Final Stage Grain Growth," *Nature*, **404**, 168–71 (2000).

[11]M. Mazaheri, A. M. Zahedi, and M. Hejazi, "Processing of Nanocrystalline 8 mol% Yttria-Stabilized Zirconia by Conventional, Microwave-Assisted and Two-Step Sintering," *Mater. Sci. Eng. A*, **492** [1–2] 261–7 (2008).

[12]M. Valefi, C. Falamaki, T. Ebadzadeh, and M. Solati-Hashjin, "New insights of The Glycine-Nitrate Process for the Synthesis of Nano-Crystalline 8YSZ," *J. Am. Ceram. Soc.*, **90** [7] 2008–15 (2007).

[13]M. I. Mendelson, "Average Grain Size in Polycrystalline Ceramics," *J. Am. Ceram. Soc.*, **52** [8] 443–6 (1969).

[14]S. Tekeli, "Fracture Toughness (KIC), Hardness, Sintering and Grain Growth Behavior of $8YSCZ/Al_2O_3$ Composites Produced by Colloidal Processing," *J. Alloys Compd.*, **391** [1–2] 217–24 (2005).

[15]G. R. Anstis, P. Chantikul, B. R. Lawn, and D. B. Marshall, "A critical Evaluation of Indentation Techniques for Measuring Fracture Toughness: I, Direct Crack Measurements," *J. Am. Ceram. Soc.*, **64** [9] 533–8 (1981).

[16]W. F. M. G. Zevert, A. J. A. Winnubst, G. S. A. M. Theunissen, and A. J. Burggraaf, "Powder Preparation and Compaction Behavior of Fine-Grained Y-TZP," *J. Mater. Sci.*, **25** [8] 3449–55 (1990).

[17]A. Ghosh, A. K. Suri, B. T. Rao, and T. R. Ramamohan, "Low-Temperature Sintering and Mechanical Property Evaluation of Nanocrystalline 8 mol% Yttria Fully Stabilized Zirconia," *J. Am. Ceram. Soc.*, **90** [7] 2015–23 (2007).

[18]I. M. G. D. Santos, R. C. M. Moreira, E. R. Leite, E. Longo, and J. A. Varela, "Sintering of Zirconia Composites Obtained by Slip Casting," *Ceram. Int.*, **27** [3] 283–9 (2001).

[19]O. Vasylkiv and Y. Sakka, "Synthesis and Colloidal Processing of Zirconia Nanopowder," *J. Am. Ceram. Soc.*, **84** [11] 2489–94 (2001).

[20]O. Vasylkiv and Y. Sakka, "Hydroxide Synthesis, Colloidal Processing and Sintering of Nano – Size 3Y-TZP Powder," *Script. Mater.*, **44** [8–9] 2219–23 (2001).

[21]A. Krell and J. Klimke, "Effects of the Homogeneity of Particle Coordination on Solid-State Sintering of Transparent Alumina," *J. Am. Ceram. Soc.*, **89** [6] 1985–92 (2006).

[22]M. Mazaheri, A. M. Zahedi, and S. K. Sadrnezhaad, "Two-Step Sintering of Nanocrystalline ZnO Compacts: Effect of Temperature on Densification and Grain Growth," *J. Am. Ceram. Soc.*, **91** [1] 56–63 (2008).

[23]A. Krell, P. Blank, H. Ma, T. Hutzler, and M. Nebelung, "Processing of High-Density Submicrometer Al_2O_3 for New Applications," *J. Am. Ceram. Soc.*, **86** [4] 546–53 (2003).

[24]M. Mazaheri, Z. R. Hesabi, and S. K. Sadrnezhaad, "Two-Step Sintering of Titania Nanoceramics Assisted by Anatase-to-Rutile Phase Transformation," *Script. Mater.*, **59** [2] 139–42 (2008).

[25]M. A. Cottom and M. J. Mayo, "Fracture Toughness of Nanocrystalline ZrO_2-3mol% Y_2O_3 Determind by Vickers Indentation," *Script. Mater.*, **34** [5] 809–14 (1996).

[26]S. Tekeli, "The Flexural Strength, Fracture Toughness, Hardness and Densification Behaviour of Various Amount of Al_2O_3-Doped $8YSCZ/Al_2O_3$ Composites Used as an Electrolyte for Solid Oxide Fuel Cell," *Mater. Design*, **27** [3] 230–5 (2006).

[27]N. Q. Minh, "Ceramic Fuel Cell," *J. Am. Ceram. Soc.*, **76** [3] 563–88 (1993).

[28]A. Selcuk and A. Atkinson, "Strength and Toughness of Tape Cast Yttria Stabilized Zirconia," *J. Am. Ceram. Soc.*, **83** [8] 2029–35 (2000).

[29]A. J. A. Winnubst, K. Keizer, and A. J. Burggraaf, "Mechanical Properties and Fracture Behaviour of ZrO_2–Y_2O_3 Ceramics," *J. Mater. Sci.*, **18** [7] 1958–66 (1983). □